How bad metals turn good: spectroscopic signatures of resilient quasiparticles Supplementary Material

Xiaoyu Deng,[1,2,3] Jernej Mravlje,[4,1,5] Rok Žitko,[5] Michel Ferrero,[1] Gabriel Kotliar,[3] and Antoine Georges[4,1,6,2]

[1] *Centre de Physique Théorique, Ecole Polytechnique, CNRS, 91128 Palaiseau Cedex, France*
[2] *Japan Science and Technology Agency, CREST, Kawaguchi 332-0012, Japan*
[3] *Department of Physics, Rutgers University, Piscataway, NJ 08854, USA*
[4] *Collège de France, 11 place Marcelin Berthelot, 75005 Paris, France*
[5] *Jožef Stefan Institute, Jamova 39, Ljubljana, Slovenia*
[6] *DPMC, Université de Genève, 24 quai Ernest Ansermet, CH-1211 Genève, Suisse*

(Dated: December 28, 2012)

PACS numbers:

SELF-ENERGY SCALING

In a Fermi liquid, $\mathrm{Im}\Sigma(\omega,T) \propto \left[\omega^2+(\pi T)^2\right]$ and therefore the self-energy obeys the following scaling in ω/T:

$$-\frac{D\mathrm{Im}\Sigma}{T^2} = A\left[\pi^2+(\omega/T)^2\right]. \qquad (1)$$

In Fig. 1, we show $-\mathrm{Im}\Sigma(\omega,T)/T^2$ as a function of ω/T for different temperatures. As the temperature is lowered below $T_{\mathrm{FL}} \approx 0.01D$, the curves collapse on a parabola, confirming the expected Fermi-liquid scaling law. Finding such a scaling is actually a stringent test on the numerical data. Very precise quantum Monte Carlo data (analytically continued with Padé approximants) and a strict control of the chemical potential were needed to obtain these results.

As the temperature is raised, the positive-frequency side quickly deviates from the scaling form, revealing a particle-hole asymmetry already for temperatures above $T/D = 0.005$. The deviations appear at a scale $\omega_+ \approx \pi T_{\mathrm{FL}}$. On the negative-frequency side the self-energy follows the quadratic behavior much more robustly and deviates from the scaling function only at about $T/D = 0.02$. Notice that the corrections on the $\omega > 0$ side grow linearly with temperature. This leads to a Seebeck coefficient which is linear in T at low temperatures, but with an enhanced slope as compared to the result one would get if these corrections were neglected.

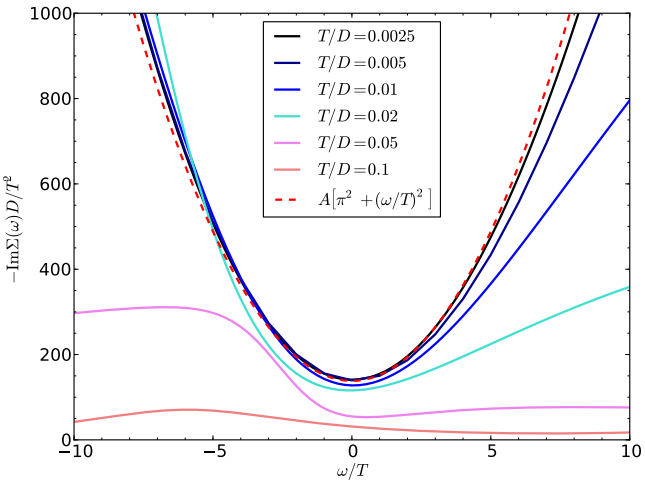

FIG. 1: The self energy scaling as ω/T for the doped Hubbard model considered in the main text (Bethe lattice, $U = 4D$, doping $\delta = 0.2$). At low temperatures self energy follows Eq. 1. A is found to be close to $Z^{-2} \sim \delta^{-2}$. (For doping 0.2, $Z = 0.22$.)

The transport probes an energy window of a few (say from -5 to 5) k_BT . In this energy window the self-energy starts to deviate appreciably at $T/D = 0.01$. This is where the resistivity (within the precision of our data) visually departs from the T^2 law.

TEMPERATURE EVOLUTION OF MOMENTUM-RESOLVED SPECTRA

In Fig. 2 we plot the temperature evolution of the momentum-resolved spectra using a color-map where bright (dark) colors indicate high (low) values of $A_k(\omega)$.

At low temperatures, the data display two peaks corresponding to: the lower Hubbard band (LHB) which disperses around $\omega_{\mathrm{LHB}} \sim -\mu_0$ and the quasiparticle peak (QP) in the vicinity of $\omega \sim 0$. μ_0 is the effective chemical potential at $T = 0$. The upper Hubbard band (UHB) centered at the energy $\omega_{\mathrm{UHB}} \sim U - \mu_0$ lies above the energy range displayed in the plot.

The lowest temperature data $T/D = 0.0025$ show a very sharp QP peak around $\omega = 0$, which is rapidly broadened as the frequency is increased. At very small frequencies, the slope of the dispersion is found to be approximately 5 times smaller than the bare one, as dictated by $Z \approx 0.2$. On the negative-frequency side this holds almost until the bottom of the band. On the positive-frequency side, instead, the kink at ω_+ is rapidly encountered. Above this kink, the slope of the band dispersion increases to about half the bare dispersion slope. The LHB, seen clearly for occupied states $k < k_F$, disperses at a slope close to that of the bare dispersion.

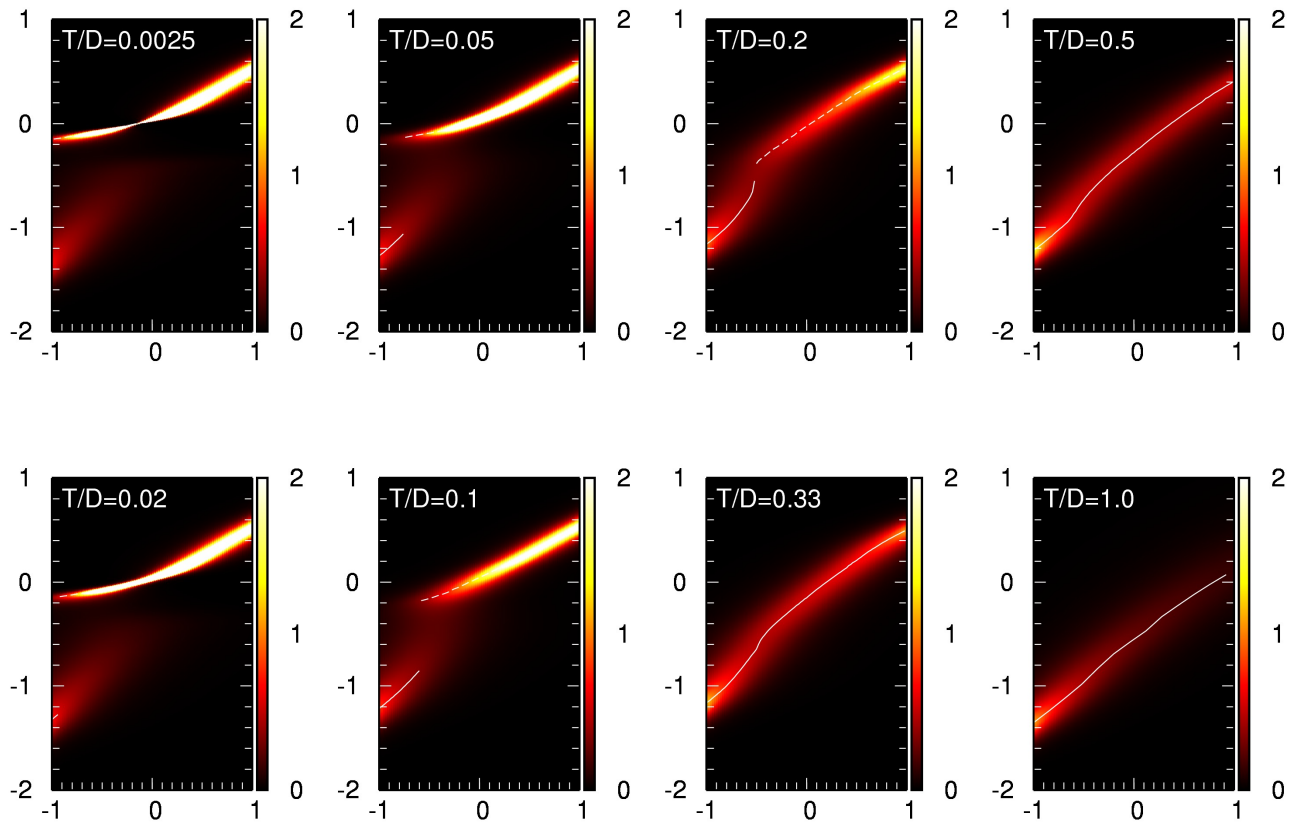

FIG. 2: Contour map of momentum-resolved spectra $A(\epsilon_k, \omega)$ at various temperatures for the same parameters as the data in the main text: doping $\delta = 0.2$ and $U/D = 4.0$.

As the temperature is increased, the QP band broadens and becomes more dispersing. It becomes therefore progressively more difficult to resolve it from the LHB band. Nevertheless, for temperatures well above $T_{\rm FL}$ and T_* (four leftmost panels) one can still clearly distinguish the QP band from the LHB. The maximum of the spectra is also indicated (lines). This maximum has a discontinuity at a point where the maximal value in the QP band becomes larger than the maximal value reached in the LHB band. Dashed and solid lines are used to denote the maximum in the QP and LHB band, respectively. Above $T/D = 0.2$ the maximal value does not have a discontinuity anymore and the signature of the quasiparticles is only visible as a kink in the dispersion. This marks the onset of the bad-metal regime. Note that $T/D = 0.2 = \delta$ corresponds to the Brinkman-Rice scale. At the highest temperature $T/D = 1.0$ the kink is not seen anymore.

The QP band crosses the Fermi energy at different momenta as the temperature increases. Identifying the Fermi surface with the momenta at which the spectral intensity of the QP band is maximal leads to the conclusion that the Fermi volume inflates as the temperature is increased. Note that the number of particles is fixed so that with this identification of the Fermi surface the Luttinger theorem is only obeyed at very low temperatures.

To elaborate on this, we plot on Fig. 3 the momentum-distribution curve at $\omega = 0$,

$$A(\epsilon_k, 0) = \frac{1}{\pi} \frac{-{\rm Im}\Sigma(0,T)}{(\mu - {\rm Re}\Sigma(0,T) - \epsilon_k)^2 + ({\rm Im}\Sigma(0,T))^2} \quad (2)$$

for several temperatures. This spectral function has the shape of a Lorentzian centered at $\mu - {\rm Re}\Sigma(0,T) - \epsilon_k$ with a width ${\rm Im}\Sigma(0,T)$. At very low temperatures a sharp peak lies at the chemical potential, fulfilling the Luttinger theorem. When the temperature increases, the peak moves to higher momenta.

An alternative way to track this change is to look at the renormalized chemical potential $\mu_{\rm eff} = \mu - {\rm Re}\Sigma(0,T)$ as a function of the temperature as shown in Fig. 4. In the Fermi-liquid regime, $\mu_{\rm eff}$ essentially follows the non-interacting chemical potential μ_0 (shown with a dashed line). At higher temperatures $\mu_{\rm eff}$ rapidly increases.

An important lesson here is that observing a well-defined QP peak does not imply that the system has

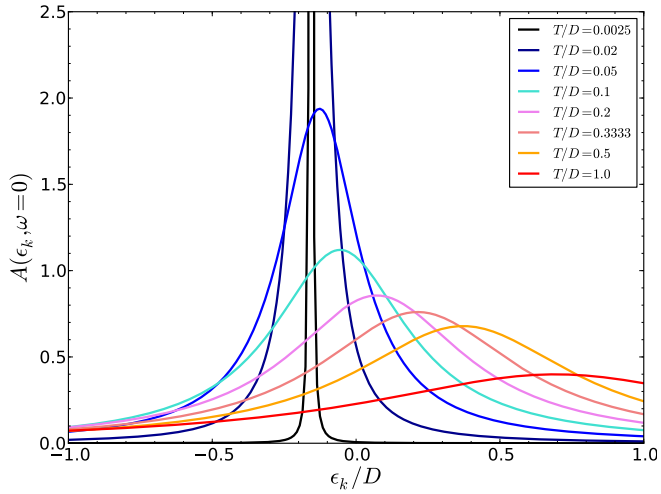

FIG. 3: The evolution of momentum-distribution curves at the Fermi level Eq. (2).

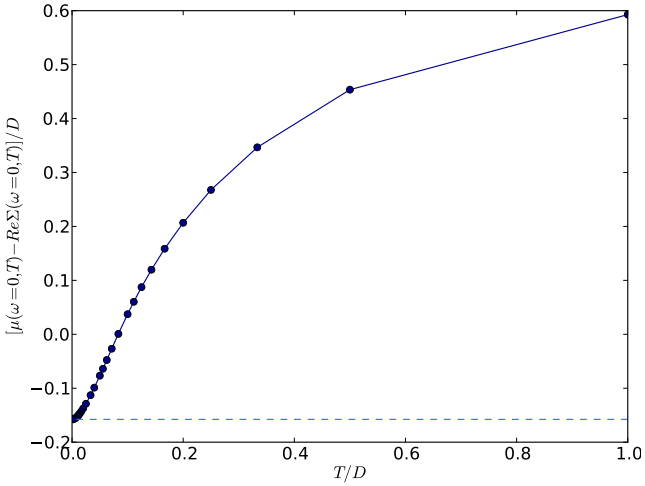

FIG. 4: Temperature dependence of $\mu_{\rm eff} = \mu(T) - {\rm Re}\Sigma(\omega = 0, T)$. The noninteracting chemical potential μ_0 is shown by a dashed line.

reached the Fermi liquid regime. As Fig. 4 shows, the chemical potential in this intermediate-temperature metal can be quite far from the Fermi energy, despite a signature of well-distinguishable resilient QPs.

THERMOPOWER AT HIGH TEMPERATURES AND COMPARISON TO APPROXIMATE FORMULAS

In Fig. 5 we show the Seebeck coefficient over a larger temperature window. The Seebeck coefficient calculated using the Kubo formula is plotted with a thick line and compared to various estimates. The Kelvin formula $\partial\mu/\partial T$ (using μ calculated within DMFT) overestimates the magnitude of the thermopower in the low-T regime

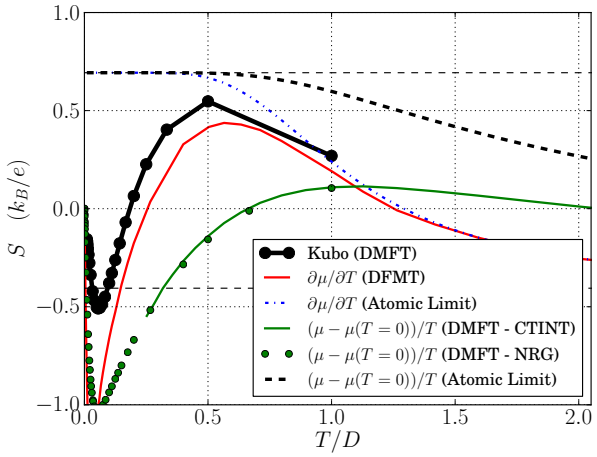

FIG. 5: Seebeck coefficient calculated using the exact Kubo formula (thick black line) compared to the approximate Kelvin formula (red line) and Heikes formula (green line and green symbols). The atomic Kelvin estimate (dotted) and Heikes estimate (thick dashed) interpolate between the asymptotic $U \to \infty$ and $U \to 0$ Heikes values.

but is a good approximation of the exact result above $T_* \approx 0.08D$. For comparison, we also plot the corresponding atomic estimate using the Kelvin formula, but using the μ obtained in the atomic limit. We note that the two expressions essentially match above $T/D = 1$. Note that the Kubo result starts to deviate significantly from the atomic estimate only when entering the resilient QP regime.

Finally, we plot Heikes estimates. The results obtained from the DMFT chemical potential using NRG and continuous-time interaction expansion Monte Carlo (CTINT) are plotted (full green line and symbols). Heikes formula is found to approximate the thermopower worse than the Kelvin formula. For comparison, also the atomic Heikes estimates (thick dashed) as well as the asymptotic $U \to 0$ and $U \to \infty$ Heikes values [1] (horizontal lines) are shown.

[1] P. M. Chaikin and G. Beni, Phys. Rev. B **13**, 647 (1976)